Journal of Marine Science and Technology

Volume 13 | Issue 2 Article 4

AN INVESTIGATION OF CONTACT PATH AND KINEMATIC ERROR OF FACE-GEAR DRIVES

Tsang-Dong Chung
Associate Professor, Department of Mechanical Engineering, Nanya Institute of Technology, Tauyan, Taiwan, R.O.C., inerchung@yahoo.com.tw

Yun-Yuan Chang
Research, Mechanical Industry Research Laboratories, Industrial Technology Research Institute (ITIR), Hsinchu, Taiwan, R.O.C.

Recommended Citation

Chung, Tsang-Dong and Chang, Yun-Yuan (2005) "AN INVESTIGATION OF CONTACT PATH AND KINEMATIC ERROR OF FACE-GEAR DRIVES," *Journal of Marine Science and Technology*: Vol. 13: Iss. 2, Article 4.
DOI: 10.51400/2709-6998.2109
Available at: https://jmstt.ntou.edu.tw/journal/vol13/iss2/4

AN INVESTIGATION OF CONTACT PATH AND KINEMATIC ERROR OF FACE-GEAR DRIVES

Tsang-Dong Chung* and Yun-Yuan Chang**

Key words: face-gear, tooth contact analysis, transmission error.

ABSTRACT

Based on the face-gear generation process, the analytical geometry of face-gear drive with its mathematical model for tooth contact analysis of face-gear and spur pinion meshing was derived. In this paper, contact path and transmission error due to assembly misalignment are analyzed by using the proposed mathematical model and the tooth contact analysis. The effects of assembly error along the axis of face-gear, misalignment of crossed and angular displacement between axes of a spur pinion and a face-gear are all investigated. The results are illustrated by several examples.

INTRODUCTION

Face-gear has been widely used in low power transmission applications. An important application of a face-gear drive is in the helicopter transmission [3]. It uses the idea of the split torque that appears to be significant where a spur pinion drives two face-gears to provide an accurate division of power. This mechanism greatly reduces the size and cost compared to conventional design.

Until now, few research activities about manufacturing and design of face-gear drive were reported. Buckingham [1] and Dudley [2] provided a brief description of face-gear drives. The research about face-gear drives was initiated by McDonnell Douglas Helicopter Co.. Important investigations of face-gear drives were performed by Litvin *et al*. [9, 10] and Litvin [3, 4]. Litvin and Egelja [5] investigated computerized generation, localization of bearing contact and simulation of meshing and contact of an orthogonal offset face-gear drive with a spur involute pinion. Two versions of geometry of face-gear drives were investigated in [7] that provides a new method for generation of face-gears by application of a grinding worm, and tooth contact analysis and stress analysis had been performed. Litvin *et al*. [6] proposed and investigated new types of face-gear drives for application in transmissions, particularly, in helicopter transmissions. Litvin *et al*. [8] developed an analytical approach for a face-gear drive with a spur involute pinion.

In this paper, numerical analysis on contact path and transmission errors induced by assembly error along axis of face-gear direction and misalignment of crossed and angular displacement between axes of face-gear and pinion is presented. It limits the results to the case of face-gear drive with the intersected axes rotation. The contents of this paper cover the following topics: (1) Generation process of face-gear by shaper with computer simulation, (2) Kinematics of face-gear meshing with spur pinion simulation, (3) Tooth contact analysis, (4) Numerical results and discussion, and (5) Conclusions.

MATHEMATIC MODEL

1. Generation process of face-gear by shaper with computer simulation

The generation process of face-gear by a shaper is illustrated in Figure 1(a). The face-gear and shaper rotates about its own axis with angular velocities, ω_2 and ω_s, respectively. Both axes intersect at point, O. Coordinate systems, $S_s(x_s, y_s, z_s)$, $S_2(x_2, y_2, z_2)$ and S_m (x_m, y_m, z_m) are respectively fixed on the shaper, face-gear, and the frame of cutting machine.

The face-gear tooth surface, Σ_2, is determined as the envelope to the family of shaper surface, Σ_s, that is represented in coordinate system, S_s. In Figure 1(b),

Paper Submitted 11/05/04, Accepted 12/31/04. Author for Correspondence: Tsang-Dong Chung. E-mail: inerchung@yahoo.com.tw.

**Associate Professor, Department of Mechanical Engineering, Nanya Institute of Technology, Tauyan, Taiwan, R.O.C.*

***Research, Mechanical Industry Research Laboratories, Industrial Technology Research Institute (ITIR), Hsinchu, Taiwan, R.O.C.*

shaper surface, Σ_s, and its position vector, $\mathbf{r_s}$, are related by

$$\mathbf{r_s}(u_s, \theta_s) = \begin{bmatrix} r_{bs}[\sin(\theta_{os}+\theta_s) - \theta_s\cos(\theta_{os}+\theta_s)] \\ -r_{bs}[\cos(\theta_{os}+\theta_s) + \theta_s\sin(\theta_{os}+\theta_s)] \\ u_s \\ 1 \end{bmatrix} \tag{1}$$

where u_s and θ_s are surface coordinates of the shaper, r_{bs} is the base circle radius of the shaper, θ_{os} determines the width of the shaper space on the base circle and can be represented by the equation

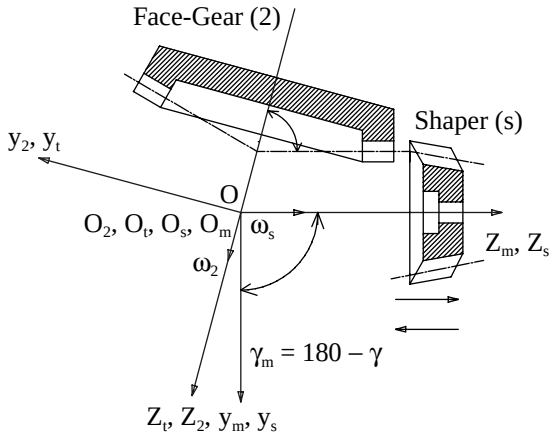

(a)

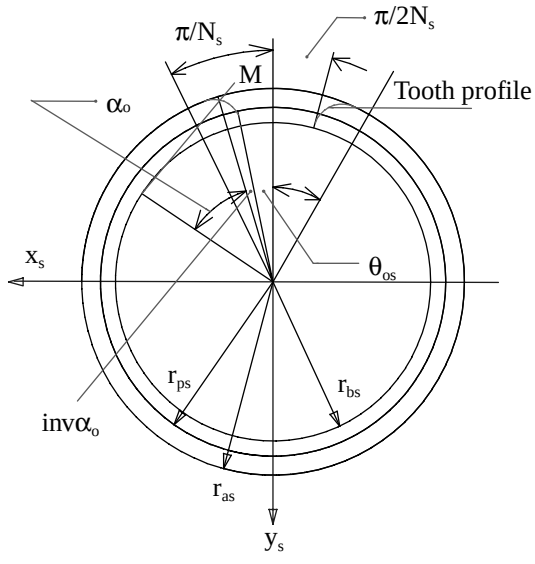

(b)

Fig. 1. (a) Face-gear generation process; (b) Shaper coordinate system.

$$\theta_{os} = \frac{\pi}{2N_s} - inv\,\alpha_o \tag{2}$$

where N_s and α_o denote tooth number and pressure angle of the shaper respectively, and *inv* is the involute function. The unit normal $\mathbf{n_s}$ to the shaper surface is given by

$$\mathbf{n_s} = \frac{\frac{\partial \mathbf{r}_s}{\partial \theta_s} \times \frac{\partial \mathbf{r}_s}{\partial u_s}}{\left|\frac{\partial \mathbf{r}_s}{\partial \theta_s} \times \frac{\partial \mathbf{r}_s}{\partial u_s}\right|} = -\begin{bmatrix} \cos(\theta_{os}+\theta_s) \\ \sin(\theta_{os}+\theta_s) \\ 0 \end{bmatrix} \tag{3}$$

The face-gear tooth surface, Σ_2, is represented in coordinate system S_2 by the following matrix equation

$$\mathbf{r_2}(u_s, \theta_s, \varphi_s) = M_{2s}(\varphi_s)\mathbf{r_s}(u_s, \theta_s) \tag{4}$$

where M_{2s} is the homogeneous transformation matrix from coordinate system S_s to S_2 by

$$M_{2s} = M_{2t}M_{tm}M_m \tag{5}$$

and where

$$M_{ms} = \begin{bmatrix} \cos\varphi_s & -\sin\varphi_s & 0 & 0 \\ \sin\varphi_s & \cos\varphi_s & 0 & 0 \\ 0 & 0 & 1 & 0 \\ 0 & 0 & 0 & 1 \end{bmatrix} \tag{5.a}$$

$$M_{tm} = \begin{bmatrix} 1 & 0 & 0 & 0 \\ 0 & \cos\gamma_m & -\sin\gamma_m & 0 \\ 0 & \sin\gamma_m & \cos\gamma_m & 0 \\ 0 & 0 & 0 & 1 \end{bmatrix} \tag{5.b}$$

$$M_{2t} = \begin{bmatrix} \cos\varphi_{2t} & \sin\varphi_{2t} & 0 & 0 \\ -\sin\varphi_{2t} & \cos\varphi_{2t} & 0 & 0 \\ 0 & 0 & 1 & 0 \\ 0 & 0 & 0 & 1 \end{bmatrix} \tag{5.c}$$

M_{ms}, M_{tm} and M_{2t} are the coordinate transformation matrices from S_s to S_m, S_m to S_t and S_t to S_2, respectively, as shown in Figures 2(a) and 2(b) and Table 1. In Figure 2(b), the auxiliary coordinate system, $S_t(x_t, y_t, z_t)$, is set up to simplify the coordinate transformation. Angle between axes z_m and z_2 is determined by $\gamma_m = 180 - \gamma$, where γ is the shaft angle of the face-gear. Rotation angles of the face-gear, φ_{2t}, and the shaper, φ_s, are related by

$$\varphi_{2t} = \varphi_s \frac{N_s}{N_2} \tag{6}$$

where N_2 denotes the tooth number of face-gear. The

equation of meshing is represented as following [3]

$$\mathbf{n_s} \bullet \mathbf{v_s}^{(s2)} = f(u_s, \theta_s, \varphi_s) = 0 \tag{7}$$

$$\mathbf{v_s}^{(s2)} = (\omega_s^{(s)} - \omega_s^{(2)} \times \mathbf{r_s} \tag{7.a}$$

where $\mathbf{v_s}^{(s2)}$, $\omega_s^{(s)}$ and $\omega_s^{(2)}$ denote respectively the sliding velocity between shaper and face-gear, angular velocities of shaper and face-gear in coordinate system, S_s. The face-gear surface in equation (4) is represented in term of θ_s, φ_s and u_s. By relating equations (4), (7) and (7.a), parameter, u_s, can be eliminated and the surface, Σ_2, can be represented by the vector function, $\mathbf{r_2}'(\theta_s, \varphi_s)$.

2. Kinematics of face-gear meshing with spur pinion

The tooth surfaces are represented by Σ_i, $i = 1$ for pinion and $i = 2$ for face-gear. In the computer simulation, it is assumed that there exist misalignments of crossed and angular displacements between two rotating axes of the mating gears, and assembly error along the axis of face-gear direction.

Coordinate systems, $S_1(x_1, y_1, z_1)$ and $S_f(x_f, y_f, z_f)$, are fixed on the pinion and the frame of the face-gear drive respectively as shown in Figures 3(a) and 3(b). In

Table 1. Transformation of coordinate systems (+): clockwise, (–): counter-clockwise

From coord. system	Rotation Axis	Rotation Angle	Translation disp.	To coord. system
S_s	z_s	$\varphi_s(-)$		S_m
S_m	x_m	$\gamma_m(+)$		S_t
S_t	z_t	$\varphi_{2t}(-)$		S_2
S_2	z_2	$\varphi_2(-)$		S_c
S_c	z_c		Δp	S_b
S_b	x_b	$\gamma_f(-)$		S_a
S_a	x_a		D	
S_a	y_a		ΔE	
S_a	z_a		$-D\cot\gamma$	S_f
S_1	z_1	$\varphi_1(-)$		S_f

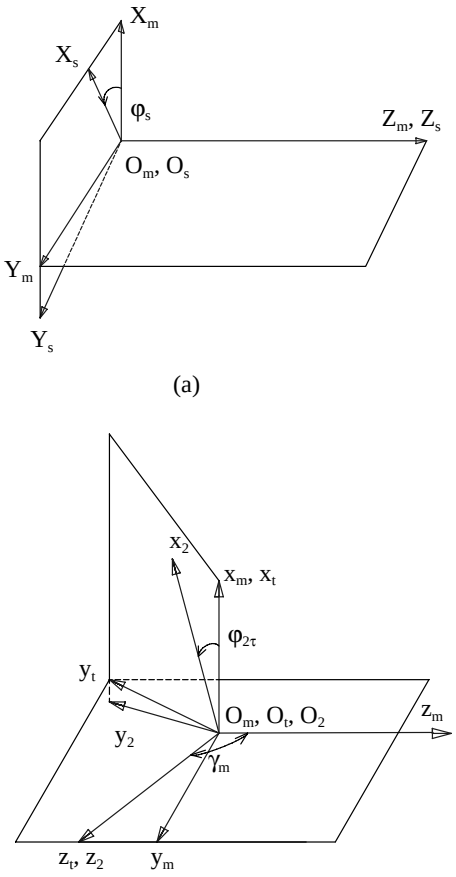

Fig. 2. (a) Coordinate systems S_s and S_m applied for generation; (b) Coordinate systems S_m, S_2 and S_t applied for generation.

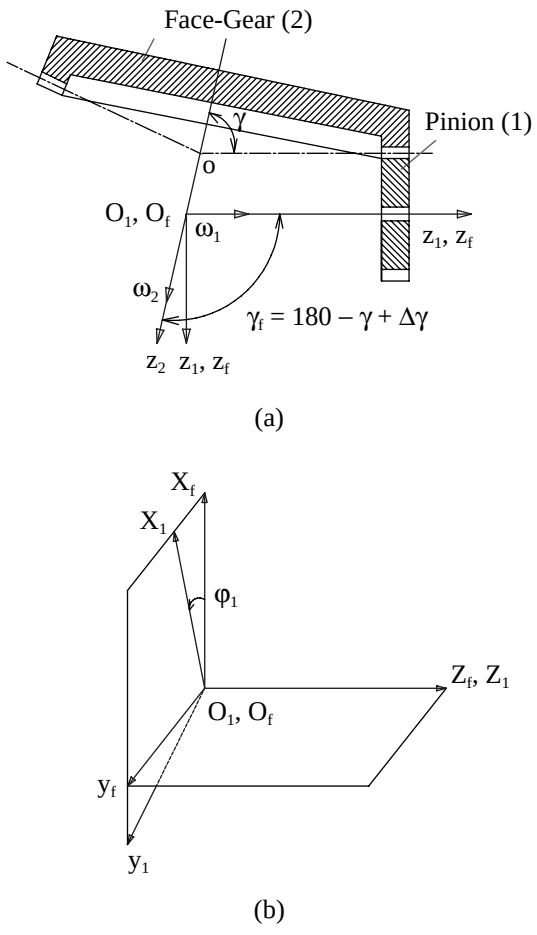

Fig. 3. (a) Pinion meshing with face-gear; (b) Coordinate systems S_1 and S_f applied for simulation of meshing.

order to simulate the misalignment of the face-gear, auxiliary coordinate systems, $S_a(x_a, y_a, z_a)$, $S_b(x_b, y_b, z_b)$ and $S_c(x_c, y_c, z_c)$, are set up in Figure 4(a). The location of Sa with respect to S_f is shown in Figure 4(b). Parameters, ΔE, D and D cot γ, determine the location of the origin O_a with respect to O_f, where ΔE is the shortest distance between the pinion and the face-gear axes when the axes are crossed but not intersected. In the following analysis, ΔE is used to simulate the crossed misalignment of the axes.

The face-gear performs rotation about axis z_2 as shown in Figures 4(c) and 4(d). The variable, Δp, along the axis of face-gear as shown in Figures 4(a) and 4(d) represents the assembly error of S_c with respect to S_b. The crossed angle, $\gamma_f = 180 - \gamma + \Delta\gamma$, is used to simulate the angular misalignment of S_b with respect to S_a and $\Delta\gamma$ is caused by the angular misalignment.

According to Figure 3(a) and Table 1, the equations of the pinion tooth surface and its unit normal can be represented in the fixed coordinate system, S_f, by applying the following coordinate transformation matrix equations:

$$\mathbf{R_f}^{(1)} = M_{f1}\mathbf{r_1} \tag{8}$$

where

$$\mathbf{r_1}(u, \theta) = \begin{bmatrix} r_b[\sin(\theta_0 + \theta) - \theta\cos(\theta_0 + \theta)] \\ -r_b[\cos(\theta_0 + \theta) + \theta\sin(\theta_0 + \theta)] \\ u \\ 1 \end{bmatrix} \tag{8.a}$$

$$M_{f1} = \begin{bmatrix} \cos\varphi_1 & \sin\varphi_1 & 0 & 0 \\ -\sin\varphi_1 & \cos\varphi_1 & 0 & 0 \\ 0 & 0 & 1 & 0 \\ 0 & 0 & 0 & 1 \end{bmatrix} \tag{8.b}$$

and

$$\mathbf{n_f}^{(1)} = L_{f1}\mathbf{n_1} \tag{9}$$

and where

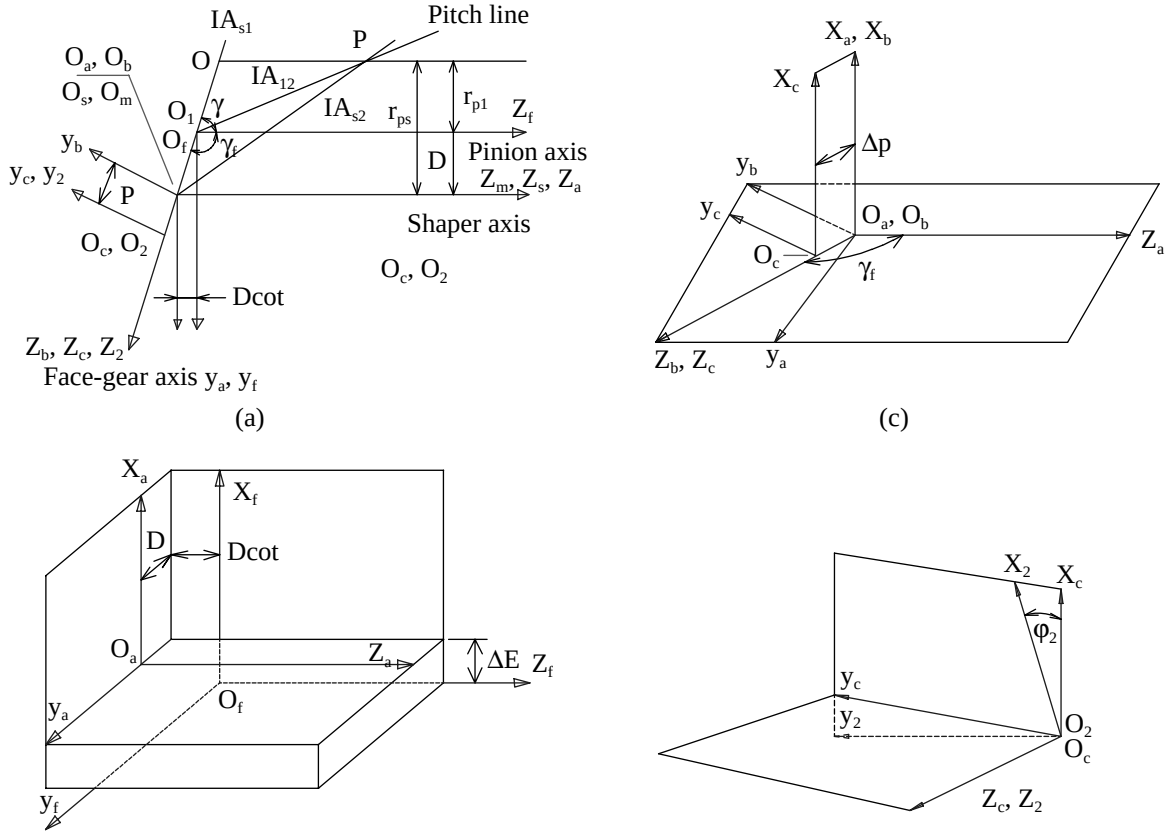

Fig. 4. (a) Relationship of coordinate systems of shaper, pinion and face-gear; (b) Coordinate systems S_a and S_f applied for simulation of meshing; (c) Coordinate systems S_a, S_b and S_c applied for simulation of meshing; (d) Coordinate systems S_c and S_2 applied for simulation of meshing.

$$\mathbf{n_1} = \frac{\frac{\partial \mathbf{r}_1}{\partial \theta_s} \times \frac{\partial \mathbf{r}_1}{\partial u_s}}{\left| \frac{\partial \mathbf{r}_1}{\partial \theta_s} \times \frac{\partial \mathbf{r}_1}{\partial u_s} \right|} = -\begin{bmatrix} \cos(\theta_o + \theta) \\ \sin(\theta_o + \theta) \\ 0 \end{bmatrix} \tag{9.a}$$

$$L_{f1} = \begin{bmatrix} \cos\varphi_1 & \sin\varphi_1 & 0 \\ -\sin\varphi_1 & \cos\varphi_1 & 0 \\ 0 & 0 & 1 \end{bmatrix} \tag{9.b}$$

Where M_{f1} and L_{f1} are the homogeneous transformation matrix and the transformation matrix from coordinate system S_1 to S_f respectively, $\mathbf{r_1}$ and $\mathbf{n_1}$ are the position vectors of pinion surface and unit normal to the surface respectively.

According to Figures 4(a) and 4(d) and Table 1, the equations of the face-gear tooth surface and its unit normal can be represented in the fixed coordinate system, S_f, by

$$\mathbf{R_f}^{(2)} = M_{f2} M_{2s} \mathbf{r_s} \tag{10}$$

where

$$M_{f2} = M_{fa} M_{ab} M_{bc} M_{c2} \tag{10.a}$$

$$M_{c2} = \begin{bmatrix} \cos\varphi_2 & -\sin\varphi_2 & 0 & 0 \\ \sin\varphi_2 & \cos\varphi_2 & 0 & 0 \\ 0 & 0 & 1 & 0 \\ 0 & 0 & 0 & 1 \end{bmatrix} \tag{10.b}$$

$$M_{bc} = \begin{bmatrix} 1 & 0 & 0 & 0 \\ 0 & 1 & 0 & 0 \\ 0 & 0 & 1 & \Delta p \\ 0 & 0 & 0 & 1 \end{bmatrix} \tag{10.c}$$

$$M_{ab} = \begin{bmatrix} 1 & 0 & 0 & 0 \\ 0 & \cos\gamma_f & -\sin\gamma_f & 0 \\ 0 & \sin\gamma_f & \cos\gamma_f & 0 \\ 0 & 0 & 0 & 1 \end{bmatrix} \tag{10.d}$$

$$M_{fa} = \begin{bmatrix} 1 & 0 & 0 & D \\ 0 & 1 & 0 & \Delta E \\ 0 & 0 & 1 & -D\cot\gamma \\ 0 & 0 & 0 & 1 \end{bmatrix} \tag{10.e}$$

and

$$\mathbf{n_f}^{(2)} = L_{f2} L_{2s} \mathbf{n_s} \tag{11}$$

and where

$$L_{2s} = L_{2t} L_{tm} L_{ms} =$$

$$\begin{bmatrix} (\cos\varphi_{2t}\cos\varphi_s + \cos\gamma_f \sin\varphi_{2t}\sin\varphi_s) & (-\cos\varphi_{2t}\sin\varphi_s + \cos\gamma_f \sin\varphi_{2t}\cos\varphi_s) & (-\sin\gamma_f \sin\varphi_{2t}) \\ (-\sin\varphi_{2t}\cos\varphi_s + \cos\gamma_r \cos\varphi_{2t}\sin\varphi_s) & (\sin\varphi_{2t}\sin\varphi_s + \cos\gamma_f \cos\varphi_{2t}\cos\varphi_s) & (-\sin\gamma_f \cos\varphi_{2t}) \\ (\sin\gamma_f \sin\varphi_s) & (\sin\gamma_f \cos\varphi_s) & (\cos\gamma_f) \end{bmatrix} \tag{11.a}$$

$$L_{f2} = \begin{bmatrix} \cos\varphi_2 & -\sin\varphi_2 & 0 \\ \cos\gamma_f \sin\varphi_2 & \cos\gamma_f \cos\varphi_2 & \sin\gamma_f \\ -\sin\gamma_f \sin\varphi_2 & -\sin\gamma_f \cos\varphi_2 & \cos\gamma_f \end{bmatrix} \tag{11.b}$$

where M_{f2} and L_{f2} are the homogeneous transformation matrix and the transformation matrix from coordinate system S_2 to S_f respectively, and L_{2s} is the transformation matrix from coordinate system S_s to S_2.

3. Tooth contact analysis

In the generation process, the surfaces of the teeth of the face-gear and the shaper are in line contact at any instant. When the pinion of the face-gear drive is identical to the shaper, the generated face-gear drive becomes sensitive to misalignment. Therefore, it is necessary to provide an instantaneous point contact between the tooth surfaces of the pinion and face-gear instead of a line contact. Therefore, the face-gear drive will be less sensitive to misalignment [9].

In Figure 4(a), IA_{s2}, IA_{s1} and IA_{12} denote respectively the instantaneous axes of rotation during meshing between Σ_s and Σ_2, Σ_s and Σ_1, Σ_1 and Σ_2. Surfaces, Σ_s and Σ_2, are in line contact at any instant in the generation process of the face-gear by the shaper. In the imaginary meshing process of the shaper and the pinion, surfaces, Σ_s and Σ_2, are in line contact at any instant. The tooth number of the shaper is usually chosen not equal but larger than the tooth number of pinion. Hence, the pinion tooth surface, Σ_1, and the generated face-gear tooth surface, Σ_2, become point contact at every instant due to the different pitch cone angles of shaper and pinion.

In order to perform the tooth contact analysis (TCA), the equations of face-gear and pinion tooth surfaces should be represented in the coordinate system S_f. At the point of contact, due to the tangency of the two gear tooth surfaces, the position vectors and their unit normals of both the face-gear and pinion tooth surfaces should be the same. Therefore, the following equations can be obtained [3]:

$$\mathbf{R_f}^{(1)} = \mathbf{R_f}^{(2)} \tag{12}$$

$$\mathbf{n_f}^{(1)} = \mathbf{n_f}^{(2)} \tag{13}$$

If equations (12) and (13) are considered simultaneously, with these equations, one has a system of five independent equations with six unknowns: φ_2, φ_1, θ, u, θ_s and φ_s, and with an additional relationship of $|\mathbf{n_f}^{(1)}| = |\mathbf{n_f}^{(2)}| = 1$. Symbols φ_2 and φ_1 denote the rotation angles of face-gear and pinion, respectively. To solve the system of equations, one of the unknowns, φ_2 may be considered as input variable to solve the five independent equations with six unknowns.

We chose φ_2 as an input variable in the practical operation, then the output rotation angle is φ_1. However, for the ideal gear meshing, the output rotation angle, φ_1, is equal to the product of input rotation angle, φ_2, and the gear ratio, N_1/N_2, that is, $\varphi_1 = \varphi_2 N_1/N_2$, where N_1 and N_2 represent the number of teeth of pinion and face-gear, respectively. From the above derivation, the relation of φ_1 and φ_2 is a nonlinear function for the practical case. The kinematic error of the gear train can be expressed as

$$\Delta\varphi_1 = \varphi_1 - \varphi_2 N_1/N_2 \tag{14}$$

where $\Delta\varphi_1$ represents the kinematic error of the gear train as a function of input variable, φ_2.

NUMERICAL RESULTS AND DISCUSSION

The analysis of contact path and kinematic error of face-gear drives is presented in this section. Some important parameters of spur pinion, face-gear and shaper chosen for this numerical example are listed in Table 2. The analysis will be limited to the case of face-gear drives with intersecting axes of rotation. Numerical examples are given below to illustrate the effects of various condition of meshing on the contact path and kinematic error.

Table 2. Some important parameters chosen for the face-gear, spur pinion and shaper

Items	Face-gear	Pinion	Shaper
Number of teeth	107	28	31
Pressure angle	25°	25°	25°
Pitch cone angle	160°	none	none
Module (mm)	3.175	3.175	3.175

In Table 3, we consider the dislocation of bearing contact for aligned face-gear drive with intersecting axes and for misalignment of ΔE = 0.1 mm between axes of face-gear and pinion. The effect of positive value of ΔE is to bring the contact points closer to the inner radius and the root of the face-gear. It leads to the less torque driving upon the gear sets and the larger load capacity for the face-gear.

The dislocated bearing contacts of axial displacement, Δp, along the axis of face-gear direction and angular misalignment, $\Delta\gamma$, of the axis of face-gear are shown in Table 4. The effects of positive Δp and $\Delta\gamma$ have opposite effect on the influence to that of positive ΔE. It results in a larger torque on the gear sets and more bending for the teeth of the face-gear.

The kinematic errors due to misalignment ΔE at the levels of 0, 0.1, 0.2 and 0.3 mm between axes of pinion and face-gear versus input rotation angle are shown in Figure 5. In this particular gear meshing, the

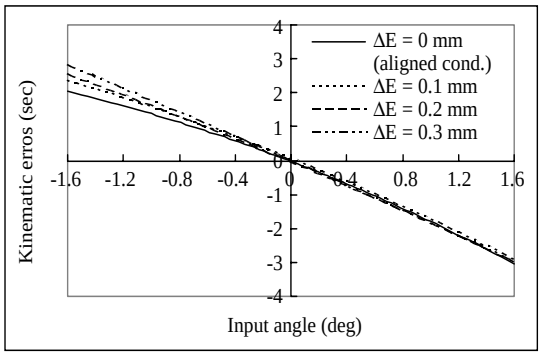

Fig. 5. The effect of the variation of the shortest distance between face-gear and pinion axes upon kinematic error.

Table 3. Contact path of ideal case and ΔE = 0.1 mm

Diff. case	Ideal case			ΔE = 0.1 mm		
ϕ_2(deg)	x_f(mm)	y_f(mm)	z_f(mm)	x_f(mm)	y_f(mm)	z_f(mm)
1.5	5.49	-42.506	192.463	5.516	-42.299	188.249
1.0	4.182	-42.986	199.625	4.199	-42.755	194.62
0.5	2.874	-43.467	208.256	2.881	-43.207	202.191
0	1.565	-43.947	218.529	1.563	-43.659	211.278
-0.5	0.256	-44.424	230.796	0.245	-44.111	222.16
-1.0	-1.053	-44.901	245.588	-1.074	-44.564	235.229
-1.5	-2.363	-45.378	263.496	-2.393	-45.013	250.895

Table 4. Contact path of Δp = 0.1 mm and $\Delta\gamma$ = 0.01 deg

Diff. case	Δp = 0.1 mm			$\Delta\gamma$ = 0.01 deg		
ϕ_2(deg)	x_f(mm)	y_f(mm)	z_f(mm)	x_f(mm)	y_f(mm)	z_f(mm)
1.5	5.727	-43.003	204.809	5.579	-42.709	197.287
1.0	4.446	-43.55	214.435	4.285	-43.227	205.656
0.5	3.163	-44.095	225.881	2.994	-43.75	215.791
0	1.88	-44.64	239.656	1.704	-44.279	228.11
-0.5	0.598	-45.185	256.341	0.417	-44.812	243.084
-1.0	-0.685	-45.728	276.611	-0.866	-45.356	261.671
-1.5	-1.969	-46.27	301.663	-2.144	-45.914	285.088

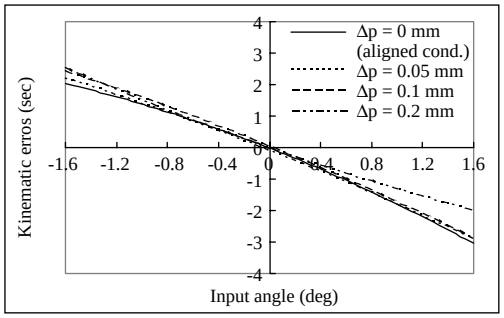

Fig. 6. The effect of assembly error along the direction of rotation axis of face-gear upon kinematic error.

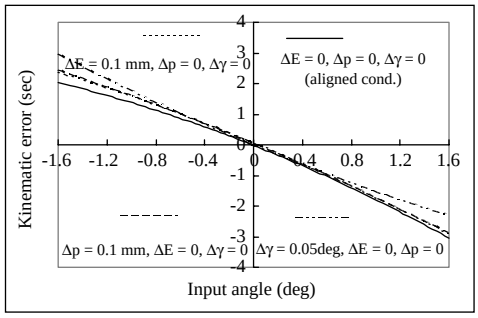

Fig. 8. The effect of angular misalignment upon kinematic error.

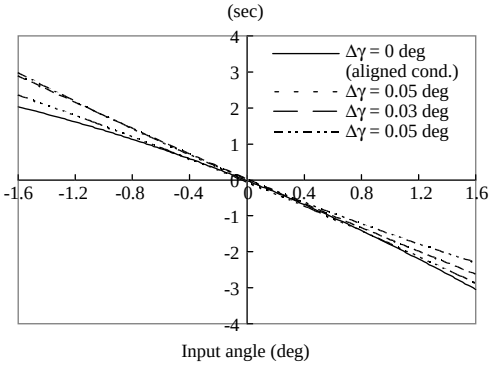

Fig. 7. The effect of angular misalignment upon kinematic error.

pinion and face-gear will contact at input angle, φ_2, from 1.6 degrees to −1.6 degrees. In the negative rotation part (0 to −1.6 degrees), larger misalignment ΔE leads to larger kinematic error. In the positive rotation part (1.6 to 0 degrees), kinematic error is relatively insensitive to misalignment.

The kinematic errors due to misalignment Δp at the levels of 0, 0.05, 0.1 and 0.2 mm along the rotation axis of the face-gear direction versus input rotation angle are shown in Figure 6. In the negative rotation part, larger misalignment, Δp, leads to larger kinematic error. In the positive rotation part, there is less effect on kinematic error due to larger value of Δp.

The kinematic errors due to angular misalignment, $\Delta\gamma$, at the levels of 0, 0.01, 0.03 and 0.05 degrees versus input rotation angle are shown in Figure 7. In the negative rotation part, larger misalignment, $\Delta\gamma$, leads to larger kinematic error. In the positive rotation part, larger assembly error leads to smaller kinematic error.

The kinematic errors due to different types of misalignment such as ΔE, Δp and $\Delta\gamma$ versus input rotation angle are shown in Figure 8. Approximately the same order of kinematic error due to misalignment is found.

CONCLUSION

From the numerical examples discussed above, some important characteristics of this type of face-gear drive can be summarized as follows:

(1) Surfaces of pinion and face-gear are in point contact in this type of face-gear drive at any instant, provided that the pinion is not identical to the shaper.
(2) The effect of positive ΔE leads to a smaller torque driving upon the gear sets and a larger load capacity

for the face-gear. The effect of positive Δp or $\Delta\gamma$ just shows the opposite behavior.

(3) Kinematic error is insensitive to the assembly error along the direction of rotation axis of face-gear, misalignment of crossed and angular displacement between axes of spur pinion and face-gear in this type of face-gear drive.

NOMENCLATURE

D Shortest distance between the axes of x_a and z_f in coordinate systems of S_a and S_f.
$K.E.$ Kinematic error.
L_{ij} Transformation matrices which transform the vector from coordinate system S_j to S_i.
M_{ij} Homogeneous transformation matrices which transform the vector from coordinate system S_j to S_i.
N_i Number of teeth of shaper, pinion and face-gear for $i = s, 1, 2$.
n_f(i) Unit normal of the pinion and face-gear tooth surfaces represented in the coordinate system $S_i (i = 1, 2)$.
$\mathbf{R_f}^{(i)}$ Position vector of the pinion, face-gear tooth surface represented in the corresponding coordinate system $S_i (i = 1, 2, f)$.
r_{as} Addendum circle radius of the shaper.
r_{bs} Base circle radius of the shaper.
r_{p1} Pitch circle radius of the pinion.
r_{ps} Pitch circle radius of the shaper.
$\mathbf{R_i}$ Position vectors of the shaper, pinion and face-gear for $\mathbf{i} = \mathbf{s}, \mathbf{1}$ and $\mathbf{2}$ in terms of variables, u_s, θ_s and φ_s.
$\mathbf{r_2}'$ Position vectors of the face-gear in terms of variables, θ_s and φ_s.
S_i Coordinate system $S (i = 1, 2, a, b, c, f, m, s, t)$.
u Gaussian coordinate of Σ_1.
u_s Gaussian coordinate of Σ_s.
$\mathbf{v_s}^{(s2)}$ Sliding velocity between shaper and face-gear.
α_o Pressure angle.
ΔE Shortest distance between the pinion and the face-gear axes.
$\Delta\gamma$ Angular misalignment of the face-gear.
Δp Axial displacement of the face-gear.
φ_i Rotation angle of shaper, pinion and face-gear for $i = s, 1, 2$.
θ Gaussian coordinate of Σ_1.
θ_s Gaussian coordinate of Σ_s.
γ Shaft angle of face-gear.
γ_f Half-cone angle of face-gear including angular misalignment.
γ_m Half-cone angle of face-gear.
S_i Tooth surface of pinion, face-gear and shaper($i = 1, 2, s$).
ω_i Rotation speed of shaper, pinion and face-gear($i = s$,

REFERENCES

1. Buckingham, E., *Analytical Mechanics of Gears*, Dover Publications, Inc., New York (1949).
2. Dudley, D.W., *Gear Handbook the Design, Manufacture, and Application of Gears*. McGraw-Hill, New York (1962).
3. Litvin, F.L., *Theory of Gearing* (PR 1212), NASA, Washington, DC (1989).
4. Litvin, F.L., *Gear Geometry and Applied Theory*, Prentice-Hall, Inc., Englewood Cliffs, NJ (1994).
5. Litvin, F.L. and Egelja, A., "Computerized Design, Generation and Simulation of Meshing of Orthogonal Offset Face-Gear Drive with a Spur Involute Pinion with Localized Bearing Contact," *Mech. Mach. Theory*, Vol. 33, pp. 87-102 (1998).
6. Litvin, F.L., Fuentes, A., and Howkins, M., "Design, Generation, and TCA of new type of Asymmetric Face-Gear Drive with Modified Geometry," *Comput. Method Appl. M.*, Vol. 190, pp. 5837-5865 (2001).
7. Litvin, F.L., Fuentes, A., Zanzi, C., and Pontiggia, M., "Design, Generation, and Stress Analysis of Two Versions of Geometry of Face-Gear Drives," *Mech. Mach. Theory*, Vol. 37, pp. 1179-1211 (2002).
8. Litvin, F.L., Fuentes, A., Zanzi, C., Pontiggia, M., and Handschuh, R.F., "Face-Gear Drive with Spur Involute pinion: Geometry, Generation by a Worm, Stress Analysis," *Comput. Method Appl. M.*, Vol. 191, pp. 2785-2813 (2002).
9. Litvin, F.L., Zhang, Y., Wang, J.C., Bossler, R.B., and Chen, J.D., "Design and Geometry of Face-Gear Drives," *ASME Trans. J. Mech. Design*, Vol. 114, pp. 642-647 (1992).
10. Litvin, F.L., Wang, J.C., Bossler, R.B., Chen, J.D., Heath, G., and Lewicki, D.G., "Application of Face-Gear Drives in Helicopter Transmissions," *Proc. International Power Transmission and Gearing Conference, ASME*, Vol. 1, pp. 267-274 (1992).